NUCL SCI TECH (2017) 28:50
DOI 10.1007/s41365-017-0199-6

Research on deposition rate of TiZrV/Pd film by DC magnetron sputtering method

Jie Wang[1] · Bo Zhang[1] · Yan-Hui Xu[1] · Yong Wang[1]

Received: 24 September 2015 / Revised: 23 November 2015 / Accepted: 8 December 2015 / Published online: 1 March 2017

Abstract An accelerator storage ring needs clean ultra-high vacuum. A TiZrV non-evaporable getter (NEG) film deposited on interior walls of the chamber can realize distributed pumping, effective vacuum improvement and reduced longitudinal pressure gradient. But accumulation of pollutants such as N_2 and O_2 will decrease the adsorption ability of the NEG, leading to a reduction of NEG lifetime. Therefore, an NEG thin film coated with a layer of Pd, which has high diffusion rate and absorption ability for H_2, can extend the service life of NEG and improve the pumping rate of H_2 as well. In this paper, with argon as discharge gas, a magnetron sputtering method is adopted to prepare TiZrV-Pd films in a long straight pipe. By SEM measurement, deposition rates of TiZrV-Pd films are analyzed under different deposition parameters, such as magnetic field strength, gas flow rate, discharge current, discharge voltage and working pressure. By comparing the experimental results with the simulation results based on Sigmund's theory, the Pd deposition rate C can be estimated by the sputtered depth.

Keywords TiZrV-Pd · Deposition rates · Magnetron sputtering method · Non-evaporable getter

1 Introduction

In order to reduce beam losses caused by residual gas scattering and to maintain a longer beam lifetime, a storage ring of a synchrotron facility needs clean ultra-high vacuum environment. The ways to obtain and maintain ultra-high vacuum are mainly through discrete distribution of vacuum pumps, such as sputtering ion pumps and titanium sublimation pumps. However, the synchrotron radiations and high-energy particles bombarding the inner wall cause surface outgassing and a high dynamic gas load. Also, due to the limitation of gas conductance of the vacuum chamber, vacuum pressure near the vacuum pumps is much better than those in other areas. TiZrV non-evaporable getter (NEG) film deposited on inner walls of the chamber can realize distributed pumping effectively, improving the vacuum by reducing both gas pressure and longitudinal gradient. With low secondary electron yield and adsorbing various kinds of gases (O_2, N_2, CO and CO_2), TiZrV films have been widely applied in particle accelerator facilities. Nevertheless, after repeated exposure to air, TiZrV films will be polluted by N_2, O_2 and so on, which reduces their absorbing behavior and service life.

When the pressure is less than 1×10^{-9} mbar, the main component of residual gas is H_2. In order to obtain ultra-high vacuum (UHV), vacuum pumps with a high pumping speed to H_2 are needed. Therefore, Benvenuti et al. [1] proposed the use of a palladium (Pd) film featuring a high adsorption of H_2 on the NEG film. The Pd film protects the NEG film and prolongs its service life. Mura et al. [2] found that TiZrV-Pd films improved the adsorption factor for other gases, too. They applied TiZrV-Pd films to ion pumps and obtained better vacuum performance. Benvenuti et al. reported that TiZrV-Pd films improved the

This work was supported by the National Natural Science Funds of China (No. 11205155) and Fundamental Research Funds for the Central Universities (WK2310000041).

✉ Bo Zhang
zhbo@ustc.edu.cn

[1] National Synchrotron Radiation Laboratory, University of Science and Technology of China, Hefei 230029, China

pumping speed for H_2 and CO, but not N_2 and CO_2. The secondary electron yield of TiZrV-Pd films caused by synchrotron radiation was lower than TiZrV films.

It has been reported that film-coating parameters in DC magnetron sputtering affect the film properties, such as film deposition rates and mechanical properties [3, 4]. In this paper, we present a study on effects of magnetic field strength, gas flow rate, discharge current, discharge voltage and working pressure on deposition rate of TiZrV-Pd films, by a magnetron sputtering deposition method.

2 Experimental

2.1 The apparatus

This magnetron sputtering deposition method is shown schematically in Fig. 1. The coating system mainly includes a pipe to be coated of Φ86 mm × 540 mm, molecular pump system, gas control system, discharge power supply, cathode wires, a sample holder and a solenoid. The cathode is of two types: twisted Ti, Zr and V wires in a total diameter of 2.5 mm and a Φ1-mm Pd wire. Details of the deposition system can be found in Ref. [3]. Film thickness was measured by a Sirion 200 Schottky field SEM (scanning electron microscope).

2.2 Methods

The deposition rate calculation and transport of sputtered particles from the target toward the walls have been discussed for decades [4–6]. The models based on continuum equations are developed to simulate the evolution of surfaces in three dimensions, and useful information is provided on morphology of step coverage for various amounts of surface diffusion and angular distributions [7]. Other models mainly rely on a kinetic Monte Carlo method. For example, the "effective thermalizing collision" (ETC) approximation has successfully explained the Keller–Simmons (K–S) formula, using an empirical equation in classical magnetron sputtering deposition with a single gas [8]. However, the models are complicated, less portable and time-consuming. According to a comparison between experimental and simulation results, we found that the deposition rate of single-component Pd metal film can be estimated by the sputtering depth for cylindrical pipe coating.

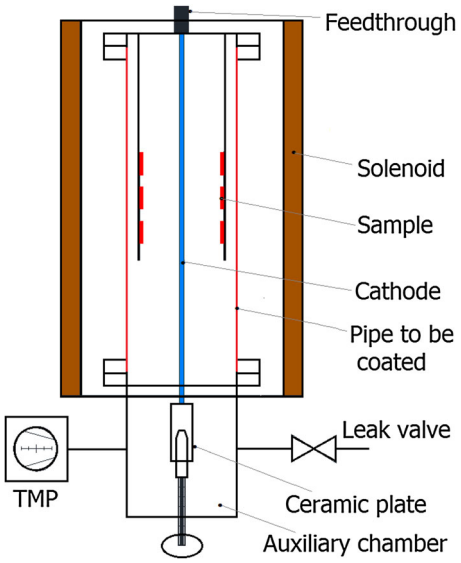

Fig. 1 Schematic diagram of the sputtering coating system

2.2.1 *Depth sputtered off the Pd target and deposition rate of the Pd film*

The depth sputtered from the Pd target, D, can be expressed as [9]:

$$D = \frac{JYr^3t}{e_0}, \tag{1}$$

where J is the beam current density, Y is the sputtering yield, t is the time of sputtering, r^3 is the volume of an atom of the target, and e_0 is the electron charge. Certainties in Y lead to certainties in the thickness scale, D. There are a number of predictive relations to calculate Y, based on Sigmund's theory [10]. In this article, we used Eq. (2) developed by Matsunami et al. [11] and Eq. (3), which was improved later from Eq. (2) by Yamamura and Tawara [12].

$$Y = \frac{0.042Q\alpha^*}{U_0}\frac{S_n(E)}{1+0.35U_0 s_e(\varepsilon)}\left(1-\left(\frac{E_{th}}{E}\right)^{1/2}\right)^s, \tag{2}$$

$$Y = \frac{0.042Q\alpha^*}{U_0}\frac{S_n(E)}{1+\frac{W\varepsilon^{-0.2}}{1+(M_1/7)^3}s_e(\varepsilon)}\left(1-\left(\frac{E_{th}}{E}\right)^{1/2}\right)^s, \tag{3}$$

where $S_n(E)$ is the nuclear stopping power per atom, U_0 is the surface binding energy per atom, $Q = 0.47$–4.6 in Eq. (2) and $Q = 0.54$–2.62 in Eq. (3), W is obtained from a lookup table provided for 34 elements, M_2 is the target atom's mass, M_1 is the incident ion mass, s is a constant, and $s_e(\varepsilon)$ is the inelastic electronic stopping power. In Eq. (2),

$$\alpha^* = 0.08 + 0.164(M_2/M_1)^{0.4} + 0.0145(M_2/M_1)^{1.29}, \tag{4}$$

and

$$E_{th} = \left[1.9 + 3.8(M_1/M_2) + 0.134(M_2/M_1)^{1.24}\right]U_0. \tag{5}$$

In Eq. (3),

$$\alpha^* = 0.249(M_2/M_1)^{0.56} + 0.0035(M_2/M_1)^{1.5},\ M_2 > M_1$$
$$= 0.0875(M_2/M_1)^{-0.15} + 0.165(M_2/M_1),\ M_2 < M_1, \quad (6)$$

and

$$E_{\text{th}} = [1 + 5.7(M_1/M_2)](U_0/\gamma),\ M_2 > M_1,$$
$$= 6.7(U_0/\gamma), M_2 < M_1, \quad (7)$$

where

$$\gamma = \frac{4M_1M_2}{(M_1 + M_2)^2}, \quad (8)$$

and, when E is in eV,

$$\varepsilon = \frac{0.03255}{Z_1Z_2\left(Z_1^{2/3} + Z_2^{2/3}\right)^{1/2}} \frac{M_2}{M_1 + M_2} E, \quad (9)$$

According to Ref. [13–15], errors of the SEM measurements are about 5%. We compared the argon ion deposition yield of Pd film obtained by Eqs. (2) and (3) with the experimental data in energy range 350–700 eV. The deposition rate C is the film thickness (T) over the deposition time (t). Adopting Wolfram Mathematica software, deposition rate of Pd film for a cylindrical pipe was calculated by the two models. Under experimental conditions given in Table 1, seven Pd film samples were deposited on silicon substrates, and the film thicknesses were measured by SEM. In the film-coating process, the discharge voltage fluctuated slightly. So, in the simulation, the discharge voltage was chosen at the relatively stable discharge voltage of the film-coating process. The simulated and measured Pd film deposition rates are given in Fig. 2a.

In most cases, the error ranges −7 to 6% for the experimental results and the values calculated using Eq. (3), and 2–11% for the experimental results and the values calculated using Eq. (3), though the largest error is 16% for both models.

Seah et al. [9] considered effects of amorphization, damage and implanted ions occurring in the early stage of sputtering and used $Q = 0.018/r^3$, where r is the average interatomic spacing. With this improvement, the Pd film deposition rates calculated using Eq. (2) deviate by −2.5 to 20% from the experiment, as shown in Fig. 2b, while they are just −7.7 to 10% for the results calculated by Eq. (3). Particularly, for samples 1, 5, 6 and 7, the errors are 0, −1.6, 0.8 and 1.6%, respectively, while for samples 2, 3 and 4, the errors are −7.7, −7.7 and 10%, respectively.

Therefore, in most cases, the deposition rate (C) is basically the same as the depth sputtered (D), which can be used to estimate the Pd film thickness.

2.2.2 *Simulation and experimental results of deposition rate*

The film thickness should be controlled in the coating process. In the early experiments, in order to obtain a preconceived film thickness, the film-coating parameters were adjusted according to the film thickness measured by SEM. In practice, to save time and cost, we calculated film thickness with the following assumptions of the empirical formula:

1. During the experiment, the current value displayed on the discharge power supply is composed of electron current and ion current. When calculating the deposition rate of Pd films, ion current is needed. In order to simplify the calculation, assume that the value of ion current is equal to the discharge current;
2. The incident energy of Ar^+ is eU, where U is the cathode voltage; and
3. The Pd films and Pd target are of the same density.

The atomic mass of Pd (m_{Pd}) sputtered by the Ar^+ and thickness of the deposited Pd film (h_{Pd}) can be calculated by:

Table 1 Parameters to prepare the seven Pd film samples on silicon substrates

Samples	Discharge current (A)	Stable discharge voltage (V)	Working pressure (Pa)	Gas flow (sccm)
#1	0.02	385	2	2.0
#2	0.02	420	2	2.0
#3	0.02	440	2	3.0
#4	0.03	500	2	2.0
#5	0.03	690	2	2.0
#6	0.04	526	2	2.0
#7	0.04	548	5	2.0

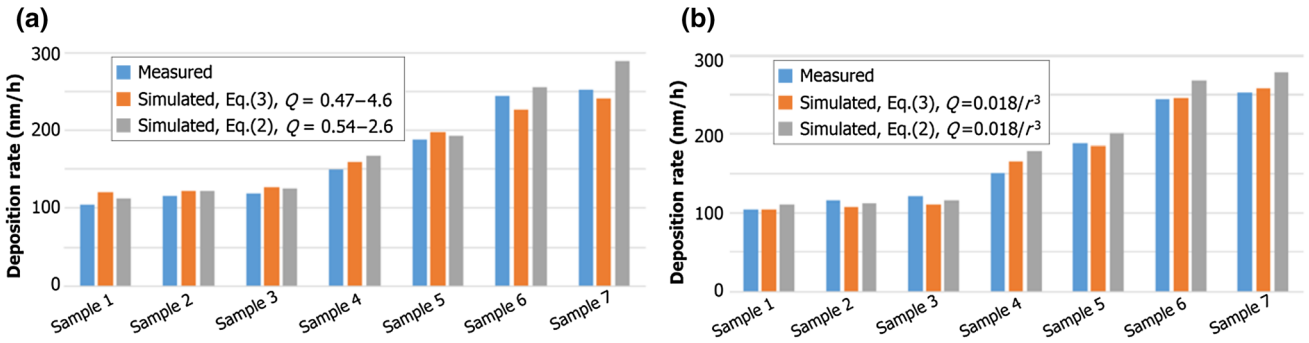

Fig. 2 Comparison of the measured Pd film deposition rates with those calculated using Eqs. (2) and (3)

$$m_{\mathrm{Pd}} = n \cdot \eta_{\mathrm{Pd}} \cdot M_{Pd}/N_{\mathrm{A}}, \quad (10)$$

$$h_{\mathrm{Pd}} = m_{\mathrm{Pd}}/(\rho_{\mathrm{Pd}} \cdot s) = n \cdot \eta_{\mathrm{Pd}} \cdot M_{\mathrm{Pd}}/(N_{\mathrm{A}} \cdot \rho_{\mathrm{Pd}} \cdot \pi d), \quad (11)$$

where $d = 0.086$ m is the pipe diameter; i is the current density in A; s is the surface area per unit length of the pipe in m^2; η_{Pd} is the Pd sputtering yields of Ar^+ in certain energies; $M_{\mathrm{Pd}} = 106.42$ g/mol is molar mass of Pd; $\rho_{\mathrm{Pd}} = 12.2 \times 10^6$ g/m^3 is the density of Pd; $N_{\mathrm{A}} = 6.02 \times 10^{23}$ mol^{-1} is the Avogadro constant; $n = i/e_0 = i \times 0.625 \times 10^{19}$ is the number of incident Ar^+ ions on the target surface in unit time.

The simulated and measured Pd film deposition rates are shown in Table 2. It can be seen that the simulation results are about 50% less than the experimental results. This means that the Pd films differ obviously in density from the Pd target. So, the depth sputtered (D) of the Pd target and deposition rate (C) of Pd films can be happen to be very close.

3 Results and discussion

The SEM was used to measure TiZrV-Pd film thicknesses deposited under different work pressures, gas flow rates, magnetic field strengths or discharge currents. In order to reduce the gas impurity effect on the film composition, the working pressure was just 1–20 Pa and the gas flow rate was just 1–5 sccm (standard cubic centimeter per minute). The discharge current was chosen based on considerations of film deposition rates. The magnetic field strength was measured by gaussmeter. The cross-sectional morphology and surface topography of some TiZrV-Pd films are shown in Fig. 3.

Table 2 The measured and simulated deposition rate (nm/h) of Pd films, assuming that the Pd target and films are of the same density

Samples	#1	#2	#3	#4	#5	#6	#7
Simulated	49	67	76	119	134	162	165
Measured	104	116	120	150	188	244	253

3.1 The influence of working pressure on deposition rates

At discharge current of 0.2 A, magnetic field strength of 120 Gauss and gas flow rate of 2 sccm, the deposition rates of TiZrV films on silicon substrates were studied under working pressure of 1–20 Pa. The results are shown in Table 3. At 2 Pa, the deposition rate of TiZrV was the highest (266 nm/h), and the discharge voltage was the highest, too.

At discharge current of 0.04 A, magnetic field strength of 175 Gauss and gas flow of 2.0 sccm, the deposition rates of Pd films on TiZrV film substrates were measured at working pressure of 2–20 Pa (Table 4). Again, at 2 Pa, the deposition rate of Pd film (244 nm/h) and the discharge voltage were the highest.

3.2 The influence of gas flow on deposition rates

At discharge current of 0.25 A, working pressure of 2 Pa and magnetic field strength of 123 Gauss, the deposition rates of TiZrV films on silicon substrate were studied at gas flow rate of 1, 3 and 4 sccm (Table 5). The highest deposition rate of TiZrV films was 278 nm/h at 1 sccm. The influence of gas flow on the deposition rates is closely related to the discharge voltage. High discharge voltage contributes to the improvement of the deposition rates of TiZrV films. This was found the same for Pd films, as shown in Table 6. At 2 sccm, the deposition rate of Pd films was the highest (240 nm/h).

3.3 The influence of magnetic field strength on deposition rates

At discharge current of 0.2 A, working pressure of 2 Pa and gas flow of 2 sccm, the deposition rates of TiZrV films on silicon substrate were studied under magnetic field

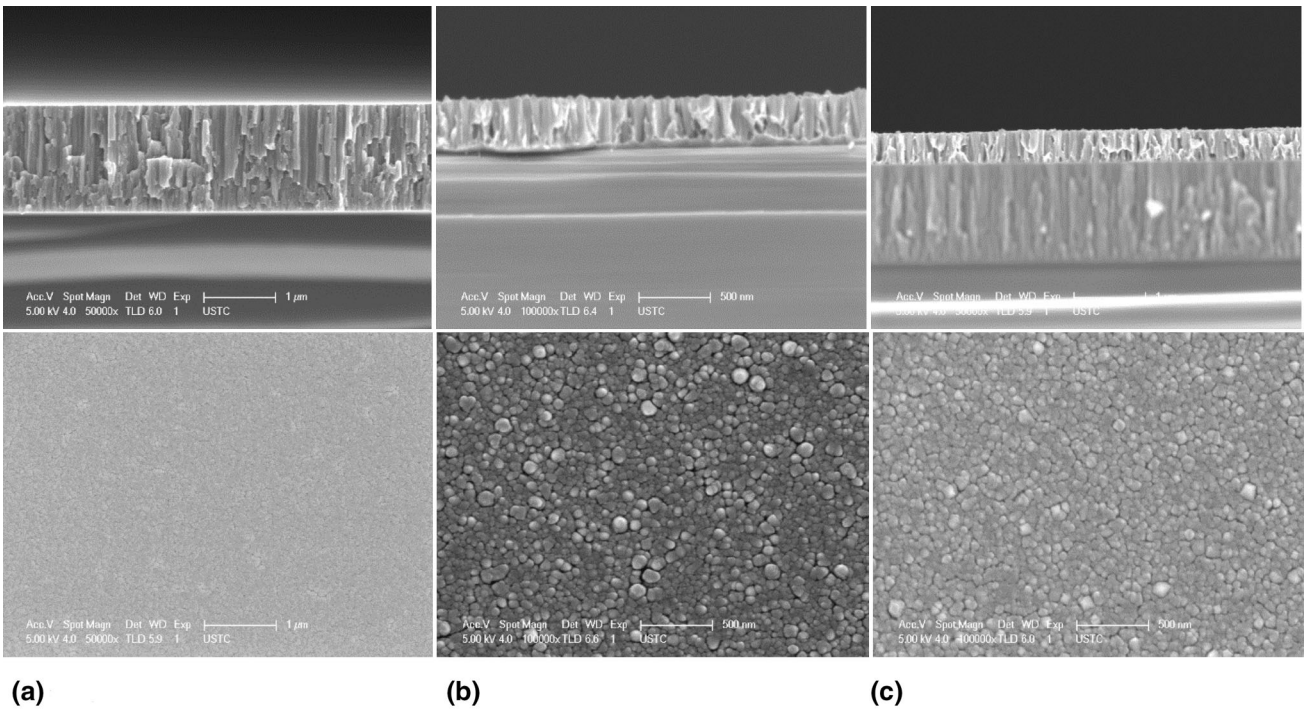

Fig. 3 Cross-sectional morphology (*upper*) and surface topography (*lower*) of #0311 TiZrV (**a**), #0227 Pd (**b**) and #0227 TiZrV-Pd (**c**) films

Table 3 Effect of working pressure on the deposition rate of TiZrV, at 0.2 A, 2.0 sccm and 120 Gauss

Samples	Working pressure (Pa)	Deposition rate (nm/h)	Discharge voltage (V)
#0610	1	260	394–365
#0311	2	266	427–436
#0527	5	147	334–319
#0604	10	170	350–314
#0612	20	139	350–329

Table 4 Effect of working pressure on the deposition rates of Pd films, at 0.04 A, 2.0 sccm and 175 Gauss

Samples	Working pressure (Pa)	Deposition rate (nm/h)	Discharge voltage (V)
#0227	2	244	530–523
#0618	5	166	437–548
#0508	10	186	456–527
#0620	20	166	464–573

Table 5 Effect of gas flow on deposition rate of TiZrV, at 0.25 A, 2.0 Pa and 123 Gauss

Sample	Gas flow (Sccm)	Deposition rate (nm/h)	Discharge voltage (V)
#0617	1	278	350–400
#0619	3	233	351–375
#0624	4	270	371–385

strengths of 82–177 Gauss (Table 7). At 82 Gauss, the highest deposition rate of TiZrV film was 500 nm/h. High discharge voltage increased the deposition rate of TiZrV film. This was found the same for Pd films (Table 8). The highest deposition rate of Pd films was 240 nm/h at 175 Gauss.

3.4 The influence of discharge current on deposition rates

At working pressure of 2 Pa, magnetic field strength of 175 Gauss and gas flow rate of 2 sccm, the deposition rates of TiZrV films on silicon substrate were studied under

Table 6 Effect of gas flow on deposition rate of Pd, at 0.02 A, 2.0 Pa and 175 Gauss

Sample	Gas flow (Sccm)	Deposition rate (nm/h)	Discharge voltage (V)
#0606	1	177	424–458
#1225	2	240	664–697
#0611	3	160	440–446
#0613	4	146	436–465
#0225	5	210	571–574

Table 7 Effect of magnetic field strength on deposition rate of TiZrV film, at 0.2 A, 2.0 Pa and 2.0 Sccm

Samples	Magnetic field strength (Gauss)	Deposition rate (nm/h)	Discharge voltage (V)
#0409	82	500	606–658
#0402	93	490	508–561
#0331	107	317	394–471
#0311	123	266	427–436
#0521	177	240	381–308

Table 8 Effect of magnetic field strength on the deposition rate of Pd film, at 0.02 A, 2.0 Pa and 2.0 Sccm

Samples	Magnetic field strength (Gauss)	Deposition rate (nm/h)	Discharge voltage (V)
#0514	65	163	443–440
#0304	123	212	559–569
#1225	175	240	664–697
#0418	206	130	430–440

Table 9 Effect of discharge current on deposition rate of TiZrV films, at 2.0 Pa, 2.0 Sccm and 175 Gauss

Sample	Discharge current (A)	Deposition rate (nm/h)	Discharge voltage (V)
#1224	0.10	30	473–490
#0108	0.25	80	547–557
#0226	0.50	316	492–343

discharge currents of 0.10, 0.25 and 0.50 A (Table 9). At 0.5 A, the deposition rate of TiZrV thin film was the highest (316 nm/h).

According to the magnetron sputtering model proposed by John A.Thornton [16], the averaged ion current J_{i_mean} can be related to the discharge current (I_{dc}) by:

$$J_{\mathrm{i\_mean}} = I_{\mathrm{dc}}/(2\pi Rw), \tag{12}$$

where R is the average radius of high-density plasma torus with a bright glow close to the cathode, and w is the width of high-density plasma torus. Ions current increases with the discharge current. According to Eq. (13), film deposition rate R_{sput} increases with ion current. Table 9 shows positive relationship between the deposition rate and discharge current, but it is not linear. Because when the discharge current increases, R and w will change slightly. In short, theoretical analysis is consistent with the experimental results.

$$R_{\mathrm{sput}} = \gamma_{\mathrm{sput}}\, J_{i\_\mathrm{mean}}/(en), \tag{13}$$

where $\gamma_{\mathrm{sput}} \sim 1$; n is the atomic density of target material.

It was found the same results hold for the influence of discharge current on the deposition rates of Pd films. When the discharge current was 0.03 A, the deposition rate of Pd film was the highest, about 217 nm/h.

4 Conclusion

The experiment results show that magnetic field strength, gas flow, discharge current and working pressure will affect the deposition rates of TiZrV-Pd films. Adjusting the four parameters and other experimental conditions, the maximum deposition rate for TiZrV thin film was 490 nm/h, and it was about 240 nm/h for Pd film. The results meet the demand of actual coating requirement. Moreover, comparing the simulation results based on Sigmund's theory and experimental results, the Yamamura and Tawaras model with $Q = 0.018/r^3$ can be used to estimate, within 10% deviation from the SEM measurement results, the deposition rate of the Pd film by the depth sputtered from the Pd target in this experiment system.

References

1. C. Benvenuti, P. Chiggiato, F. Cicoira et al., Vacuum properties of palladium thin film coatings. Vacuum **73**, 139–144 (2004). doi:10.1016/j.vacuum.2003.12.022
2. M. Mura, C. Paolini, Use of getter-catalyst thin films for enhancing ion pump vacuum performances. J. Vac. Sci. Technol. A **25**, 1234 (2007). doi:10.1116/1.2731348
3. J. Wang, B. Zhang, Y.H. Xu et al., Deposition and characterization of TiZrV-Pd thin films by dc magnetron sputtering. Chin. Phys. C **39**, 127007 (2015). doi:10.1088/1674-1137/39/12/127007
4. K. Meyer, I.K. Schuller, C.M. Falco, Thermalization of sputtered atoms. J. Appl. Phys. **52**(9), 5803 (1981). doi:10.1063/1.329473
5. A. Gras-Marti, J.A. Valles-Abarca, Slowing down and thermalization of sputtered particle fluxes: energy distributions. J. Appl. Phys. **54**(2), 1071 (1983). doi:10.1063/1.332113
6. G.H. Gilmer, H. Huang, C. Roland, Thin film deposition: fundamentals and modeling. Comput. Mater. Sci. **12**, 354–380 (1998). doi:10.1016/S0927-0256(98)00022-6
7. J. Li, J.P. McVittie, J. Ferziger et al., Optimization of intermetal dielectric deposition module using simulation. J. Vac. Sci. Technol., B **13**, 1867 (1995). doi:10.1116/1.587826
8. J.H. Keller, R.G. Simmons, Sputtering process model of deposition rate. IBM J. Res. Dev. **23**, 24 (1979). doi:10.1147/rd.231.0024
9. M.P. Seah, An accurate semi-empirical equation for sputtering yields, II: for neon, argon and xenon ions. Nucl. Instrum. Methods Phys. Res. B **229**, 348–358 (2005). doi:10.1016/j.nimb.2004.12.129
10. P. Sigmund, Theory of sputtering. I. Sputtering yield of amorphous and polycrystalline targets. Phys. Rev. **184**, 383 (1969). doi:10.1103/PhysRev.184.383
11. N. Matsunami, Y. Yamamura, Y. Itikawa et al., Energy dependence of the ion-induced sputtering yields of monatomic solids. Atom. Data Nucl. Data Tables **31**, 1 (1984). doi:10.1016/0092-640X(84)90016-0
12. Y. Yamamura, H. Tawara, Energy dependence of ion-induced sputtering yields from monatomic solids at normal incidence. Atom. Data Nucl. Data Tables **62**, 149 (1996). doi:10.1006/adnd.1996.0005
13. GB/T 16594-2008. General rules for measurement of length in micron scale by SEM
14. GB/T 20307-2006. General rules for nanometer-scale length measurement by SEM
15. GB/T 16594-1996. Micron grade length measurement by SEM
16. J.A. Thornton, Magnetron sputtering: basic physics and application to cylindrical magnetrons. J. Vac. Sci. Technol. **15**(2), 171–177 (1978). doi:10.1116/1.569448